Appl. Phys. B 72, 361–366 (2001) / Digital Object Identifier (DOI) 10.1007/s003400100474

Applied Physics B
Lasers
and Optics

Angle-dependent THz tomography – characterization of thin ceramic oxide films for fuel cell applications

M. Brucherseifer[1,*], P. Haring Bolivar[1], H. Klingenberg[2], H. Kurz[1]

[1] Institut für Halbleitertechnik II, RWTH Aachen, 52056 Aachen, Germany
[2] Institut für Technische Physik, DLR, 70569 Stuttgart, Germany

Received: 8 June 2000/Revised version: 13 September 2000/Published online: 10 January 2001 –

Abstract. A time-resolved THz tomography system for the incidence-angle-dependent three-dimensional characterization of layered structures is presented. The capabilities of the developed system are demonstrated on multi-layer ceramic samples used for solid oxide fuel cells (SOFC). Appropriate methods for determining unknown refractive indices are discussed. It is shown how the angle of incidence of a THz imaging system has a significant influence on measured signals. This fact can be exploited especially in Brewster-angle configurations to enhance the capabilities of any THz tomography system. Data evaluation algorithms are presented.

PACS: 42.30.Wb; 81.70.Fy; 78.47.+p

Since the emergence of time-resolved THz imaging, many interesting applications have been demonstrated [1–6]. The imaging techniques developed to date rely on the spatially resolved analysis of either transmitted [1] or reflected [5] optically generated THz pulses. This paper focuses on the second alternative, namely the time- and spatially resolved detection of reflected THz pulses, which permits the three-dimensional tomographic analysis of the internal structure of objects. A new THz tomography setup is presented, which permits incidence-angle-dependent measurements. It is shown how the angle of incidence of the THz pulses has a significant influence on the observability of the internal structure of analyzed samples. This dependency can be exploited, especially in Brewster-angle configurations, to enhance the general capabilities of any THz tomography system.

The characterization capabilities of the developed THz tomography setup are demonstrated on multi-layered ceramic oxide structures used for solid oxide fuel cells (SOFC). SOFC have an enormous potential for power generation applications. Nevertheless, no non-destructive quality control system for their sensitive manufacturing process exists to date. We will show that the developed THz imaging system can fulfill this role and by that means aid the breakthrough of this attractive technology.

The paper is structured as follows: Section 1 introduces SOFC and describes the samples investigated. Section 2 describes the THz tomography system developed and discusses appropriate methods for determining unknown refractive indices. Section 3 outlines the THz characterization of SOFC – analysis of single layer and multi-layered ceramic oxide samples are presented. Section 3 also discusses the data analysis algorithms employed.

1 Investigated samples – solid oxide fuel cells

SOFC represent a promising future energy supply system due to their high overall efficiency and low emission of pollutants. SOFC technology is currently under development for a broad spectrum of power generation applications [7]. However, before SOFC can be introduced onto the market several technical challenges remain to be solved. Production costs are still not competitive and need to be reduced significantly. In this context it is therefore of primary importance to develop efficient characterization methods to control and optimize manufacturing processes.

A schematic cross-section of a typical SOFC is depicted in Fig. 1. The ceramic fuel cell consists of two electrodes (the anode and the cathode) separated by a solid electrolyte such as yttria-stabilized zirconia (YSZ). Typical thickness are in the 10–100 μm range. Fuel (e.g. H_2) is fed to the anode, generally consisting of a Ni/YSZ cermet, and releases electrons in an electrochemical oxidation reaction to the external circuit. Oxidant (e.g. O_2) is fed to the cathode, consisting of a perovskite-type material, where it undergoes a reduction reaction by accepting electrons from the external circuit. The solid electrolyte conducts ions between the two electrodes. Such a single cell typically produces a voltage of approximately 1 V at the operating temperature of 850–950 °C. Thus, for practical applications SOFC are connected in electrical series (stacks) to provide higher voltages. The bipolar plates

*Corresponding author. (E-mail: brucherseifer@iht-ii.rwth-aachen.de)

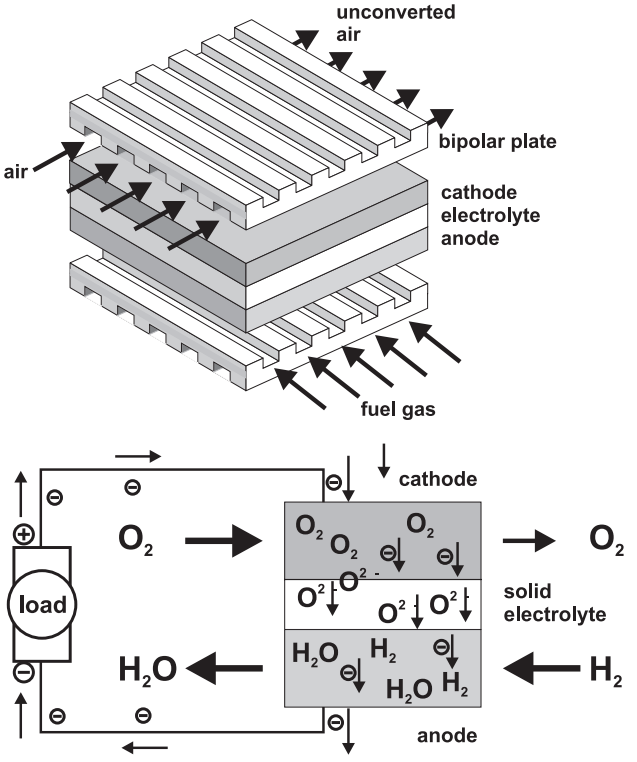

Fig. 1. A schematic cross-section of a solid oxide fuel cell. Typical ceramic oxide layer thicknesses are on the order of a few tens of micrometers

which connect the anode of one cell to the cathode of the next in a stack additionally act as a supply channel for the reacting gases.

The manufacturing process for this type of SOFC is extremely demanding: An excellent control of the porosity and dimensions of all layers is required since an efficient transport of molecular gases in the anode and cathode is required, while the electrolyte has to transport only ionized species and be completely impermeable to molecular gas. Despite these technical difficulties and the wide potential application of SOFC, currently, no appropriate characterization system for these layered ceramic oxide structures exist. Conventional optical approaches fail in this opaque and highly scattering materials – acoustic tomography lacks the necessary spatial resolution. To date the standard analytic procedure is to cut SOFC samples, polish them and then analyze the structures under conventional or electron microscopes.

In this paper we show the application of time-resolved terahertz (THz) tomography for the efficient characterization of fuel cell structures. The following experimental analysis demonstrates the plausibility of using this technique as a flexible and non-destructive means for quality control and online monitoring of the manufacturing process in order to aid the breakthrough of this attractive technology. Two different types of samples will be presented: The first test samples consists of only one layer of YSZ film plasma sprayed onto a metallic Ni/ZrO_2 anode. These samples are used to test the analytic capabilities of the THz system and develop adequate tools for determining unknown refractive indices. The second type of samples are complete three-layer SOFC structures deposited on flat bipolar substrates. All analyzed samples were manufactured by vacuum plasma spraying at the DLR in Stuttgart, Germany [8].

2 THz tomography setup

The general idea of a THz tomography system is to perform a time-resolved measurement of THz pulses reflected from a sample. As in a simple time-of-flight measurement (ToF), time delays of THz reflections at interfaces correlate with the depth from which the reflections originate. If the propagation constants of the THz pulse are known, i.e. if the refractive index profile is known, one can determine the vertical profile of a sample. The spatial resolution in the two lateral dimensions can then be achieved either by using a focused THz pulse and sequentially measuring reflected signals and scanning the object within the focal plane [1] or by measuring in parallel the reflection of a broadened parallel THz beam [2, 3].

The experimental setups used for our analysis are depicted in Fig. 2. Femtosecond laser pulses from a commercial Ti:sapphire laser system are used both to generate THz pulses in a surface field emitter and to detect them by gating a photoconductive THz antenna. The THz pulses are focused on the sample and the reflected radiation onto the detection antenna with parabolic metallic mirrors. The lateral resolution is attained by moving the analyzed object in the focal plane of the setup. The temporal evolution of the reflected signal is scanned with a fast shaker system. An AIXScan data acquisition system (40 MHz sampling rate) allows the rapid acquisition of complete THz transients. Integrated digital signal processors (DSP) permit the online automated analysis of the measured data.

Two configurations are employed to allow a flexible variation of the incidence angle of the THz tomography system: The first configuration, depicted in the upper part of Fig. 2, allows samples to be analyzed under precise normal incidence by utilizing a pair of polarizing beamsplitters (metallic gratings). This approach, while frequently used in far-infrared Fourier transform spectroscopy [9], has not been applied for time-resolved THz spectroscopy experiments previously. The second setup, schematically represented in the lower part of Fig. 2, allows THz tomographic analysis under variation of the angle of incidence of the THz pulses.

A necessary step before being able to interpret THz tomographic images is the determination of the refractive index profile $n(z)$ of the analyzed samples. This is of special importance, as material properties in the THz frequency regime are frequently unknown. For the analyzed ceramic material systems, we find that the usual calculation [5] of the refractive index from reflection coefficients via Fresnel equations $[r = (n_1 - n_2)/(n_1 + n_2)]$, does not yield reliable results. This approach is problematic since long-term fluctuations of the laser system and the surface and interface textures of the sample affect the detected reflection amplitudes. In addition, unknown absorption coefficients also considerably influence measured amplitudes. Using THz amplitude information to determine the refractive coefficient profile is therefore problematic.

An alternative to using THz reflection amplitudes to determine refractive indices is the measurement of time delays in a sample with a well-known geometry, e.g. a sample

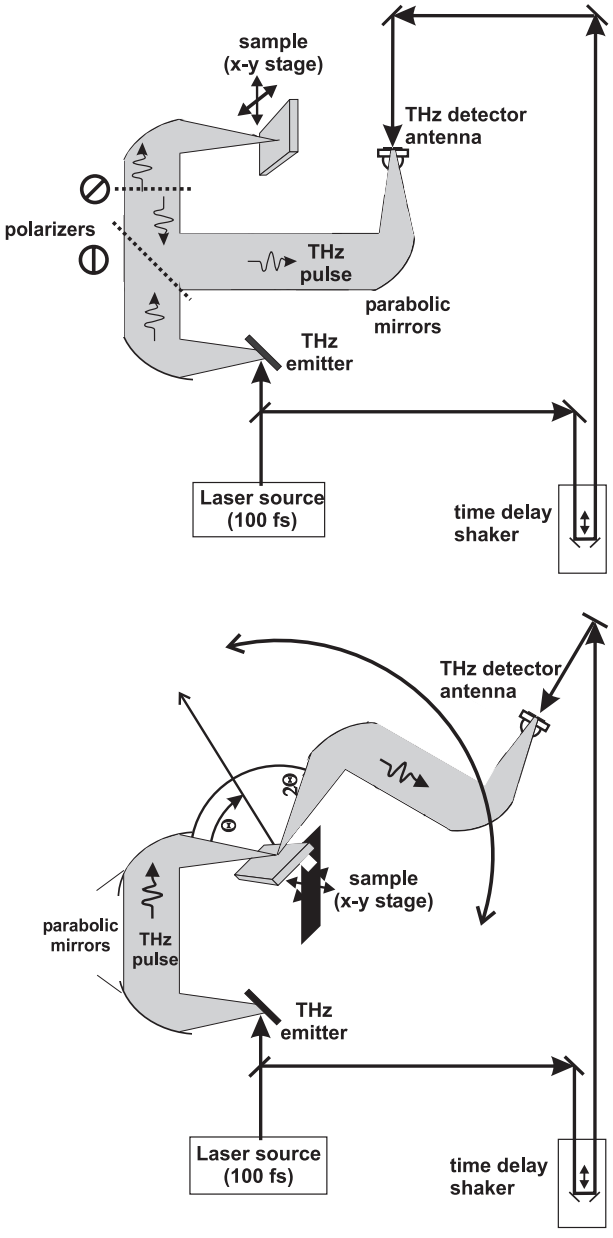

Fig. 2. Two complementary setups for THz tomography. The spatial resolution is achieved by moving the sample in the focal plane of the THz imaging system. The *upper setup* is designed for the examination of samples under normal incidence. The *lower setup* allows the angle of incidence of the THz pulses to be varied

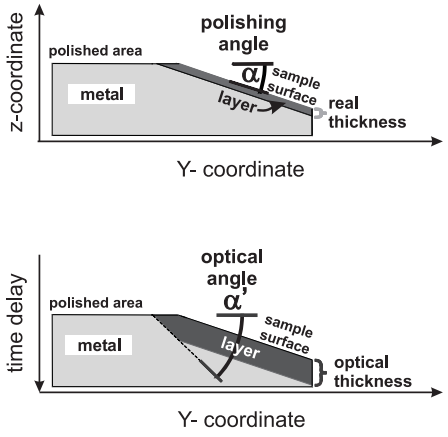

Fig. 3. Scheme of the refractive index measurements. The *upper figure* depicts the cross-section of a layered sample polished at a defined angle, the *lower figure* the time delay experienced by the THz pulses, i.e. the optical thickness. The refractive index can easily be calculated from the ratio of the slopes of the polishing angle α and the slope of the time delay (optical angle α') of the back-side reflex in the transition region

with a known layer thickness. When the dimensions are not precisely known, a simple approach can be applied to circumvent this problem in layered structures: The basic idea is to polish an edge of the sample under a small angle, as depicted in Fig. 3. It is important to use a polishing angle substantially smaller than the system's aperture (here 30°), in order to collect the full reflected signals despite their propagation direction change. The upper part of the figure depicts a schematic cross-section of a single-layer sample that was polished at a small angle from top to bottom. The lower part of the figure depicts the corresponding time delay at which reflections of the different interfaces appear (THz pulses are assumed to enter from the top of the figure). As THz pulses that are reflected from the front surface travel exclusively through air ($n_{\text{air}} = 1$), the detected time delay exactly reproduces the shape of the surface. However, if THz pulses are transmitted through a layer, their velocity becomes slower due to the higher refractive index of the layer. They therefore need a longer time to traverse this layer, which thus appears thicker in the time domain. Due to simple continuity considerations, this leads automatically to a different optical-delay slope for the back-side reflection (layer–metal interface) in the transition region where the real thickness of the layer increases. It is clear that the refractive index n of the layer can then be determined from the ratio of the back-side reflection slope (α') in the transition region to front-side reflection slope (α). Since only homogeneity in the transition region has to be presupposed, this method for determining refractive indices is less problematic than previous approaches.

Figure 4 shows experimental data for a sample of YSZ film plasma sprayed onto a metallic Ni/ZrO_2 anode. This test sample is polished as described before. A THz reflection line scan is taken across the polished interface region under normal incidence. The amplitude of the THz transients at each temporal position (vertical axis) and y coordinate (horizontal axis) is depicted on a gray scale map. The measured peak positions (light areas) clearly resemble the expected positions for the interfaces, as illustrated already in Fig. 3. In the region where the thickness of the layer is constant, the lines of the back-side and front-side reflections are parallel. In the transition region, where the layer thickness increases, the slope of the back-side reflection is steeper. The ratio of both slopes allows the refractive index of the YSZ film to be determined. Equivalent line scans are measured at several positions along the interface (x coordinate), and the respective refractive indices are also calculated. These values are depicted in the lower part of Fig. 4. The error bars illustrate that the 5% variation of the determined values is dominated by authentic variations of the refractive index, given, for example, by an inhomogeneous density (porosity discrepancy) of the YSZ film.

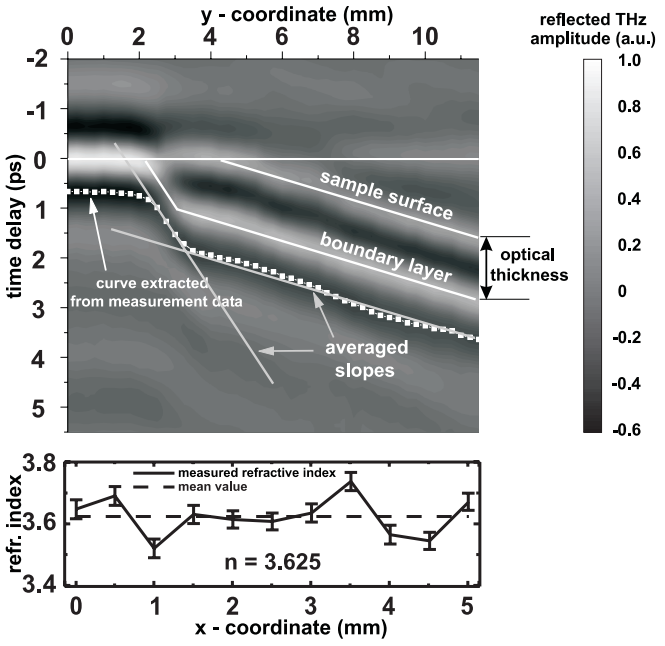

Fig. 4. The *upper figure* depicts a THz line scan of a single-layer perovskite sample. Individual THz transients are taken on a line across the polished interface region (y coordinate).The *gray scale* indicates the reflected THz field amplitudes at the respective time delay. The *lower figure* depicts the refractive index extracted from several of such line scans at different positions along the interface (x coordinate)

3 Characterization of solid oxide fuel cells

Here, the first demonstration of the analytic capabilities of THz imaging is made on a single-layer sample consisting of an YSZ film plasma sprayed onto a metallic Ni/ZrO_2 anode. Such a film is typically used as the electrolyte layer in SOFC structures. A two-dimensional scan of THz reflection transients is taken with the normal-incidence setup depicted in the upper part of Fig. 2. Assuming an average value for the refractive index of $n = 3.6$ from the previous analysis, one can readily determine the thickness of the YSZ film at a given point, from the temporal distance of the front-side and back-side reflections. Figure 5 shows the ascertained spatially resolved map of the thickness of this YSZ film. One can clearly recognize the strong variation (more than 50%) of the layer thickness. The observed concentrically structured thickness variation is presumably caused by an inhomogeneous temperature distribution during the plasma deposition of the layer, indicating an insufficient thermal coupling of the substrate. This measurement exemplifies the capability of THz tomography in monitoring the properties of the deposited ceramic layer. THz imaging can thus aid in the control and further development of the manufacturing process of this type of materials for SOFC applications.

In a further step, a complete SOFC sample consisting of three ceramic layers on a metal substrate is analyzed with the THz tomography system. The metallic substrate is made from $CrFe_5Y_2O_{31}$. The anode, electrolyte and cathode are deposited in this order by plasma spraying them onto the metallic substrate. The layers consist respectively of $NiZr_2$ cermet, YSZ and LaSr perovskite. The sample is polished at a small angle of approximately 1.5° to determine the refractive indices of the three layers. In order to obtain the best possible spatial resolution, we adopt again the normal incidence configuration, as depicted in the upper part of Fig. 2. As before, line scans of THz reflection transients across the polished section are taken. Such a line scan is shown in Fig. 6.

Reflections from the sample surface (at delay times around 0 ps) as well as from the surrounding sample mount (at $\approx$10 ps) can clearly be identified. The slope on the right side of the front-side reflection indicates the polishing angle. However no reflections from the interface layers are visible. The only slight additional THz amplitude fluctuations visible in Fig. 6 are artifacts (ghost images of the front-side reflex) related to residual water absorption and internal reflections in the THz source. The absence of any reflections from internal layer interfaces is mainly due to the extremely strong reflection at the surface. Only a small part of the THz pulse is coupled into the sample; hence, the small reflections from the interfaces are overshadowed by the measurement artifacts, which are mainly due to the water absorption of the strong surface reflex. Decreasing this surface reflex also decreases these artifacts and hence increases the visibility of internal reflections.

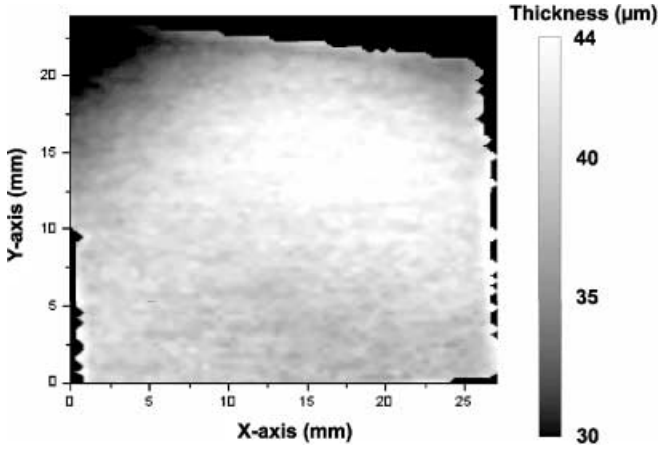

Fig. 5. THz tomographic measurement of the spatially resolved thickness of a YSZ film. The concentric thickness variation seems to indicate a temperature gradient in the substrate during the plasma spraying of the layer

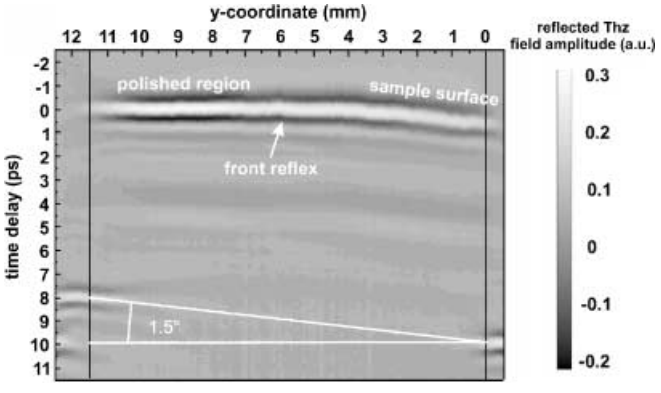

Fig. 6. THz line scan of the three-layer SOFC structure, taken under normal incidence to optimize spatial resolution. Only reflections at the front interface can be observed

This result illustrates that the three-layer SOFC sample requires a more elaborate analysis to discern the individual layers of the more complex structure. A first enhancement of the analytic capabilities of the system is attained by decreasing the surface reflection and therefore increasing the coupling of the THz pulse into the sample. For this purpose, a different reflection geometry is adopted, in order to be able to vary the angle of incidence of the THz pulses, as depicted in the lower part of Fig. 2. Evidently, when the incidence angle matches the Brewster angle of the front surface, the sensitivity for the detection of internal structures increases dramatically. A line-scan measurement at the Brewster angle is presented in Fig. 7. As expected, reflections from the back sides of all layers can now easily be identified, despite the still present artifacts of the measurement. Comparing this measurement to the previous one in Fig. 6 demonstrates that the variation of the angle of incidence of a THz imaging system can be exploited advantageously to enhance the capabilities of any THz tomography system to selectively detect specific structures of the analyzed objects.

From Fig. 7 one can also see that the refractive indices of the layers do not differ by much; this is evident from the similar slopes of the back-side reflection in the transition regions of the layers. The small refractive index change partially explains the difficulty in detecting the respective interfaces – the main reason which prevented discernment of the internal structure is nevertheless the ghost artifacts. In order to reduce the influence of these artifacts and extract only the features of the measurement which are of further interest, an additional refinement of the analytic method is necessary: By applying adaptive filtering [10] to the measured data, a reference mirror reflection signal, exhibiting the same characteristic temporal shape (including the ghost artifacts), is deconvoluted from the measurement data. This numerical analysis not only eliminates the ghost artifacts, but additionally drastically enhances the attainable contrast and dynamic range of the THz tomographic imaging system. In order to illustrate this effect, Fig. 8 presents a comparison of a simple peak detection algorithm applied to the as-measured data (upper plot) and to the data after adaptive filtering (lower plot). In the former case, no threshold peak value can be found to discern real reflections from ghost artifacts. However, after elimination of the ghost artifacts by adaptive filtering, the peak positions of the front-side and back-side reflections can readily be determined.

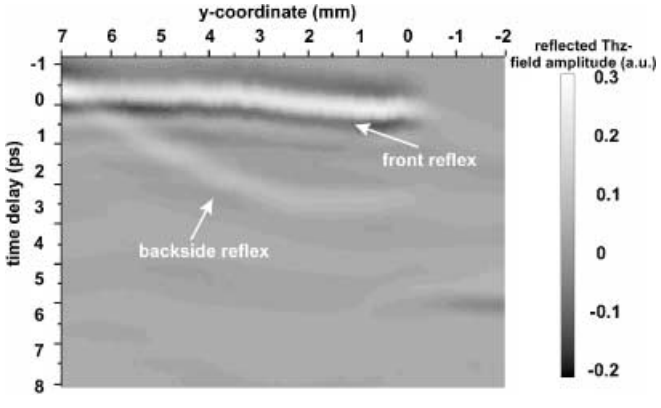

Fig. 7. THz tomographic line scan of the three-layer SOFC structure taken at a Brewster angle. This configuration minimizes front interface reflections and hence increase the non-coupled part of the THz radiation. The reflections from the back sides of all three layers are now readily observable

Table 1. Refractive indices and thicknesses of the three layers in the analyzed SOFC cross-sectio

Layer	Function	Refractive index	Thickness (μm)
1	Anode	2.25	29
2	Electrolyte	4.08	31
3	Cathode	4.11	42

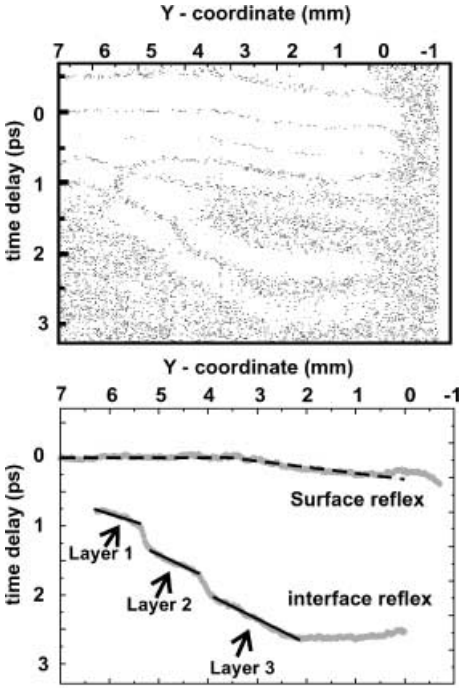

Fig. 8. Comparison of different data extraction algorithms. The *upper plot* shows a standard peak detection analysis of the measured data. The *lower plot* shows the analysis after adaptive filtering in order to reduce noise, eliminate artifacts and extract only the surface and back-side reflections

As shown previously, having identified the interface reflections and respective slopes in the adaptively filtered data, it is straightforward to determine the refractive indices and dimensions of the ceramic oxide layers of the SOFC sample. Table 1 presents, as an example, the results for this particular cross-section of the sample. This analysis exemplifies again the capability of time-resolved THz tomography as a powerful tool for the non-destructive characterization of these attractive multi-layered material systems. In the future, we wish to enhance the spatial resolution of the imaging system, in order to increase the capability to characterize SOFC structures and be able to identify small defects (voids and inhomogeneities) in the 10–100 μm range [11].

4 Conclusions

This paper presents a time-resolved THz imaging system for the incidence-angle-dependent three-dimensional

tomographic analysis of layered structures. The capabilities of the developed system are enhanced in a sequence of consecutive improvements. The application of this tomographic system to the non-invasive efficient analysis of multi-layer ceramic samples used for high temperature solid oxide fuel cells (SOFC) is demonstrated. Methods for measuring unknown refractive indices are discussed. It is shown that the angle of incidence dependence of a THz imaging system can be exploited especially in Brewster-angle configurations to enhance the capabilities of any THz tomography system. The importance of numerical post-processing of the measured data is exemplified and discussed.

Acknowledgements. We would like to thank R. Henne and T. Henne (DLR Stuttgart) for providing and preparing the SOFC samples. We acknowledge financial support by the Deutsche Forschungsgemeinschaft under contract number DFG Ku 340 / 37-1.

References

1. B. B. Hu, M.C. Nuss: Opt. Lett. **20**, 1716 (1995)
2. P.U. Jepsen, C. Winnewisser, M. Schall, V. Schyja, S.R. Keiding, H. Helm: Phys. Rev. E **53**, 3052 (1995)
3. Q. Wu, T.D. Hewitt, X.-C. Zhang: Appl. Phys. Lett. **69**, 1026 (1996)
4. D.M. Mittleman, J. Cunningham, M.C. Nuss, M. Geva: Appl. Phys. Lett. **71**, 16 (1997)
5. D.M. Mittleman, S. Hunsche, L. Boivin, M.C. Nuss: Opt. Lett. **22**, 904 (1997)
6. M.C. Nuss, J. Orenstein: In *Millimeter and Sub-Millimeter Wave Spectroscopy of Solids*, ed. by G. Grüner (Springer, Heidelberg 1998) p.7–50
7. N.Q. Minh, T. Takahashi, *Science and Technology of Ceramic Fuel Cells* (Elsevier, Amsterdam 1995)
8. R. Henne, G. Schiller, V. Borck, M. Müller, M. Lang, R. Ruckdäschel: Int. Thermal Spry Conf., Nice, France **2**, 933 (1998)
9. D.H. Martin, E. Puplett: Infrared Phys. **10**, 105 (1970)
10. H.D. Lüke: *Signalübertragung* (Springer, Berlin 1991)
11. S. Hunsche, M. Koch, I. Brener, M.C. Nuss: Opt. Commun. **150**, 22 (1998)